Pergamon

Int. J. Heat Mass Transfer. Vol. 39, No. 13, pp. 2683–2697, 1996

0017-9310/96 $15.00 + 0.00

0017-9310(95)00351-7

Cooperating thermosolutal convection in enclosures—II. Heat transfer and flow structure

D. GOBIN and R. BENNACER†

Fluides, Automatique et Systèmes Thermiques, URA 871, Laboratoire de l'Université Pierre et Marie Curie associé au CNRS, Campus Universitaire, Bât. 502, 91405 Orsay Cedex, France

(*Received* 27 *January* 1995 *and in final form* 26 *September* 1995)

Abstract—This paper reports the numerical simulations of double diffusive natural convection flows in a binary fluid contained in a two-dimensional enclosure, with imposed horizontal temperature and concentration differences between the vertical walls. The analysis concerns the influence of the different parameters governing the problem in the heat transfer characteristics and on the flow structure. The study is focused on steady-state solutions in the cooperating situation. At high Lewis numbers, numerical simulations show that heat transfer decreases with increasing buoyancy ratios. This phenemenon is analysed on the basis of the flow structure, and a scale analysis is provided to estimate the decrease in heat transfer. Then, the influence of the parameters on the formation of a multicellular flow structure is discussed.

1. INTRODUCTION

Natural convection in enclosures with both temperature and concentration horizontal gradients has received growing attention in the last few years, but numerical studies on heat transfer for high Lewis number fluids are still few, and correlations for heat transfer as a function of the governing parameters (Grashof numbers, Lewis number) in such situations are scarcely found in the literature. Some numerical results in the low Lewis number range (that is, $Le \approx 1$) have been obtained by Bénard *et al.* [1], Lin *et al.* [2] or Béghein *et al.* [3]. Situations at high Lewis numbers ($Le \approx 100$) have been investigated by Han and Kuehn [4] in the steady-state, or Lee and Hyun [5] in the transient regime, and the simulation results show the existence of multicellular flow structures under the condition of moderately high buoyancy ratio ($N = Gr_S/Gr_T$). This confirms a number of experimental observations showing that thermosolutal natural convective flows exhibit multicellular structures for moderate values of the buoyancy ratio and for various values of the aspect ratio:

(1) Kamotani *et al.*, [6], ($Le = 300$, $A < 1$, $Gr_S \sim 10^6$), have observed multicellular regimes for $N > 10$ in the cooperating situation and for $N < -6$ when the buoyancy forces are in opposition.

(2) Lee *et al.* [7], ($Le = 100$, $A = 2$, $Gr_S \sim 10^7$, also report such observations for $8 < N < 55$ in the cooperating case and for $-13 < N < -5$ in the opposing situation.

(3) Han and Kuehn [4], ($Le = 250$, $A = 4$, $Gr_S \sim 10^6$), similarly show the existence of multiple cells for cooperating buoyancy forces ($10 < N < 50$) and for opposing terms ($-10 < N < -2$).

The numerical results presented hereafter concern a large range of parameters and allow for the study of the heat transfer and the flow structure in a more systematical way. This work is intended to give more insight into the formation of the multicellular regime and on its impact on the heat transfer characteristics.

The mathematical formulation of the problem and the characteristics of the numerical method have been described in the companion paper and are not repeated here. The following section presents a discussion of the heat transfer results in such systems, and the study is then dedicated to a presentation of the multicellular flow regime.

2. HEAT TRANSFER

The set of numerical simulations reported in the companion paper is analysed in this section in terms of heat transfer. Let us first recall the range of parameters that has been considered in this study:

$$\begin{cases} A = 1 \\ Pr = 7 \\ Gr_T \in [10^3\text{–}10^6] \\ N \in [0.1\text{–}100] \\ Le \in [1\text{–}1000]. \end{cases} \quad (1)$$

2.1. *Influence of* N

Figure 1 presents the average wall heat transfer ($\overline{Nu}$) at a thermal Grashof number $Gr_T = 10^5$, as a function of the buoyancy ratio N, and for different

† Present address: IUSI, rue d'Eragny, 95031 Neuville-sur-Oise, France.

NOMENCLATURE

A	aspect ratio of the enclosure, H/L
Gr_S	solutal Grashof number based on H, $g\beta_S\Delta CH^3/\nu^2$
Gr_T	thermal Grashof number based on H, $g\beta_T\Delta TH^3/\nu^2$
h^*	height of stratification zone
h_C	height of the thermal cell
H (L)	height (width) of the enclosure
Le	Lewis number: Sc/Pr
N	buoyancy ratio: Gr_S/Gr_T
$\overline{Nu}$	average Nusselt number (dimensionless heat flux)
Pr	Prandtl number, ν/α
Sc	Schmidt number, ν/D
$\overline{Sh}$	average Sherwood number (dimensionless mass flux)
$x(z)$	dimensionless coordinate, $x^*/H(z^*/H)$.
β_S	coefficient of volumetric expansion with concentration
ΔC	concentration difference between plates, C_2-C_1
ΔT	temperature difference between plates, T_2-T_1
δ_T	thermal boundary layer thickness
δ_S	solutal boundary layer thickness
ν	kinematic viscosity
μ	viscosity
ϕ	dimensionless concentration: $(C-(C_2+C_1)/2)/\Delta C$
ξ	dimensionless height of the stratified zones
ρ	fluid density
θ	dimensionless temperature: $(T-(T_2+T_1)/2)/\Delta T$.

Greek symbols

α	thermal diffusivity
β_T	coefficient of volumetric expansion with temperature

Subscripts

H	based on H
S	solutal
T	thermal.

values of the Lewis number. The observation of the results leads to the following remarks:

(1) At a given value of the thermal Grashof number and for the low values of N, the Nusselt number is almost constant and insensitive to the Lewis number; it remains close to the value corresponding to pure thermal natural convection, since the solutal buoyancy term is almost negligible ($N/Le \ll 1$).

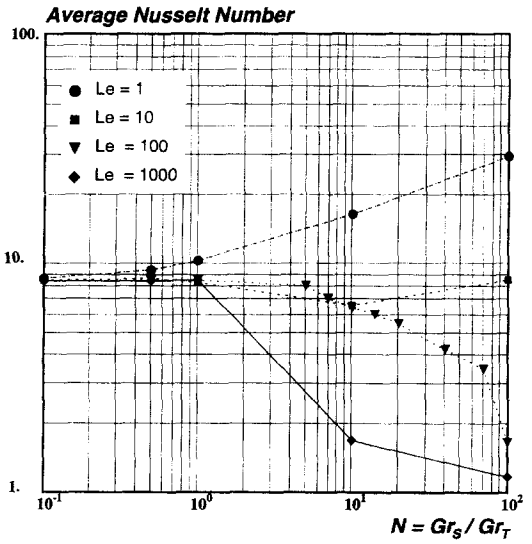

Fig. 1. Influence of N on the average Nusselt number ($A = 1$; $Pr = 7$; $Gr_T = 10^5$).

(2) At high values of the buoyancy ratio, the variation of $\overline{Nu}$ with N drastically depends on the Lewis number.

(a) At the *low* Le values, $\overline{Nu}$ *increases* with N. This corresponds to the usual fact that when the source term in the Navier–Stokes equation increases (N is positive), the convective flow is enhanced, and the resulting heat transfer increases: this is what has been assessed in the companion paper concerning mass transfer. This is also confirmed by the heat transfer correlations in the low Le range proposed by the previous studies available in the bibliography, [2, 8, 9].

(b) At the *high Le* values ($Le = 100$ or $Le = 1000$), $\overline{Nu}$ *decreases* with increasing N, and the Nusselt number tends towards a value of 1, that is, towards *diffusive* heat transfer. The same conclusion may be obtained from the analysis of the results at $Gr_T = 10^3$, 10^4 or 10^6 [11]. Similar observations have been reported in previous numerical studies by Hyun and Lee [10] or Han and Kuehn [4], and require a deeper analysis.

Indeed this result is in contradiction with what could be expected; when the solutal buoyancy force strongly dominates over the thermal term ($N = 100$) at high Lewis numbers (100 and more) thermosolutal natural convection results in *quasi-diffusive heat transfer* ($\overline{Nu} \simeq 1$). In order to illustrate this observation, more detailed results are displayed in Fig. 2(a–c) for $N = 50$, $Gr_T = 10^3$, $Le = 100$ and $Pr = 7$. At such high values of N and Le, the density of the binary fluid

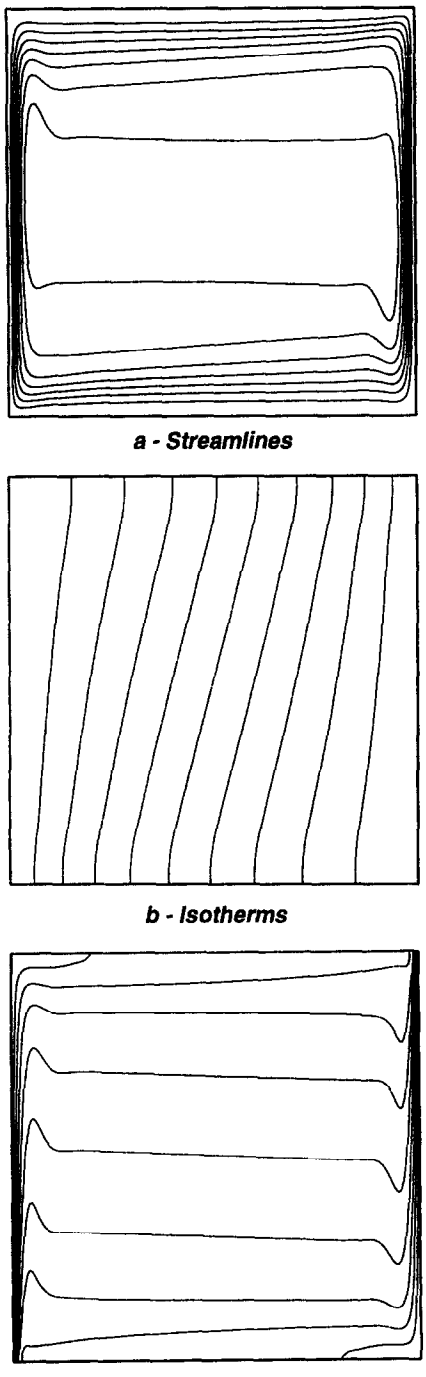

Fig. 2. Structure of the (a) velocity, (b) temperature (c) concentration fields ($A = 1$; $Pr = 7$; $Le = 100$; $Gr_T = 10^3$; $N = 50$): (a) $\Delta\psi = 0.1$; (b) $\Delta\theta = 0.1$; (c) $\Delta\phi = 0.1$.

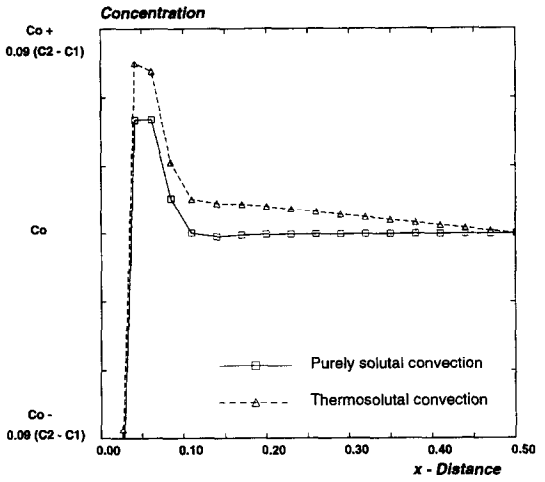

Fig. 3. Concentration profiles in the horizontal midplane ($A = 1$; $Pr = 7$; $Gr_S = 5 \times 10^4$; $Le = 100$). (a) $Gr_T = 0$; (b) $Gr_T = 10^3$.

mainly depends on the local concentration field; the flow concerns a very thin boundary layer along the walls of the enclosure [Fig. 2(a)], and the concentration is stratified over the whole height of the cavity [Fig. 2(c)]. Nevertheless, it may be seen in Fig. 2(b) that the isotherms are almost parallel to the vertical walls, indicating that the temperature field is not affected by the flow and that the heat transfer in the enclosure is purely conductive.

It must be emphasized that if only the corresponding thermal conditions were imposed (no solutal effect in the source term of the Navier–Stokes equation), the heat transfer would be dominated by thermal natural convection ($\overline{Nu} = 2.01$). This confirms the paradox that *enhancing* the buoyancy term through the solutal component ($N = 50$) reduces the heat transfer to such an extent that convection does not participate in heat transfer.

In order to provide an interpretation of this result, the concentration profiles in the horizontal midplane are compared in Fig. 3 for two situations: the thermosolutal flow and the purely solutal solution (same parameters as Fig. 2, Gr_S in unchanged, but Gr_T is set to 0). It may be seen that, although very similar, the two profiles exhibit some significant differences, especially outside of the solutal boundary layer. The velocity profiles (not shown) confirm that, at such a high N value, the flow is driven by the solutal buoyancy force, and that the thermal buoyancy term only weakly modifies the flow due to purely solutal convection. However, the linear horizontal distribution of the temperature field shown in Fig. 2(b) should induce a buoyancy force far from the solutal boundary layer, in the central part of the cavity where the concentration field is stratified. It may be seen on the figure that the concentration profile in the core in the thermosolutal case is slightly inclined compared to the purely solutal profile, so that the solutal buoyancy term locally balances the source term due to the temperature field. It may be verified that the horizontal concentration gradient in the centre of the cavity is such that $\Delta C/\Delta X \simeq 1/N(\Delta T/L)$.

These observations show that the origin of the heat transfer decay with increasing N at high Le for a given thermal Grashof number is due to the fact that very little energy is advected on the scale of the velocity

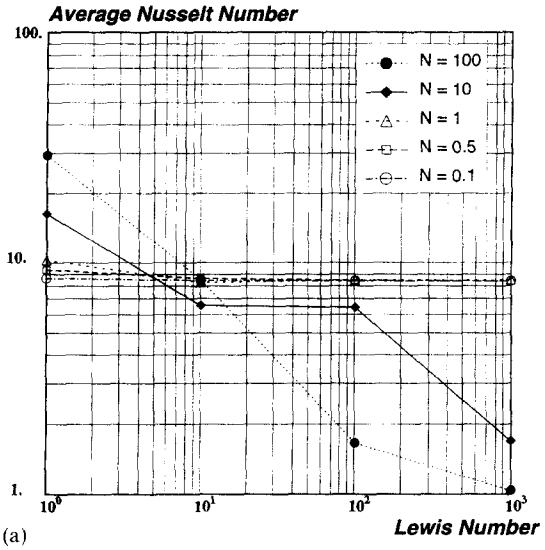

(a)

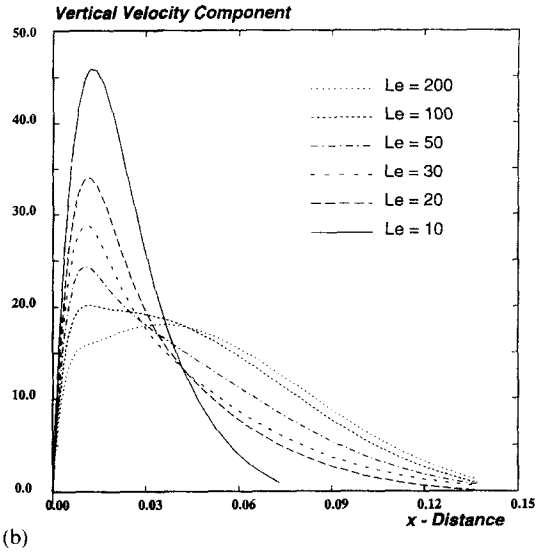

(b)

Fig. 4. Influence of the Lewis number ($A = 1$; $Pr = 7$; $Gr_T = 10^5$); (a) on the average Nusselt number, (b) on the vertical velocity component in the horizontal midplane ($N = 20$).

boundary layer, and that the buoyancy term that would be created in the core of the cavity by the linear (diffusive) temperature distribution is locally balanced by a slight correction of the concentration field.

2.2. *Influence of* Le

Also of interest is the variation of the Nusselt number for different values of the Lewis number at given values of the thermal and solutal Grashof numbers (Gr_T and N fixed). Figure 4(a) shows the average heat transfer variations with the Lewis number for different values of N ($Gr_T = 10^5$, $Pr = 7$, $A = 1$). The figure clearly shows that $\overline{Nu}$ remains relatively constant at low N values ($N \leqslant 1 : N/Le \ll 1$); thermal convection is dominant, and the Nusselt number keeps the value corresponding to the (constant) thermal Grashof number, as it has been observed in Fig. 1. At higher N values ($N = 10$ or $N = 100$) two main differences may be observed:

(1) at low Lewis numbers, the Nusselt number is significantly higher than in the thermally driven situation;

(2) the Nusselt number decreases with increasing Le, and for the highest values of the Lewis number, it gets close to 1, corresponding to negligible influence of convection on heat transfer.

This latter influence is illustrated by the vertical velocity profiles in the horizontal midplane in the vicinity of the left wall at $N = 20$ [Fig. 4(b)]. The figure shows that the vertical velocity component decreases with increasing Le, leading to a lower heat transfer. The velocity reduction associated with the increase of the Lewis number is not in contradiction with the increase of *mass transfer* observed in the companion paper: indeed the Lewis number is increased through the Schmidt number, and this effect dominates over the reduction of the solutal boundary layer thickness.

It is useful to recall that the analysis is based on a boundary layer description of the velocity, temperature and concentration fields close to the vertical walls. The main conclusion of the heat transfer analysis presented above is that the results are not in agreement with the usual scales, except at low values of N or Le. This may arise from the fact that the boundary layer approximation is not valid in the high N-high Le range as far as the temperature field in concerned.

In Figure 5(a–c), the main fields are plotted for a situation where the Nusselt number is lower than the value that could be expected from a boundary layer analysis ($Gr_T = 10^5$, $N = 20$, $Le = 100$). The isotherms, streamlines and isoconcentration lines have a quite particular aspect that may contribute to the explanation of the decrease of the Nusselt number:

(1) The flow is limited to the central part of the cavity [Fig.5(a)], and the top and bottom regions of the enclosures are almost 'stagnant' zones, characterized by very low fluid velocities.

(2) The concentration field is characterized by extremely thin boundary layers, and while the central convective cell has an homogeneous concentration [Fig. 5(c)], the solute mass fraction in the top and bottom zones is stratified.

(3) The temperature field is also consistent with the flow structure [Fig. 5(b)]. The central cell is stratified in temperature, while the isotherm distribution in the regions adjacent to the horizontal walls is parallel to the vertical walls, indicating a conduction-like behaviour, due to the fact that the fluid in these regions is practically motionless.

These remarks justify the interest of analysing the effect of N and Le on the flow structure and of studying the concentration stratification in the top and bot-

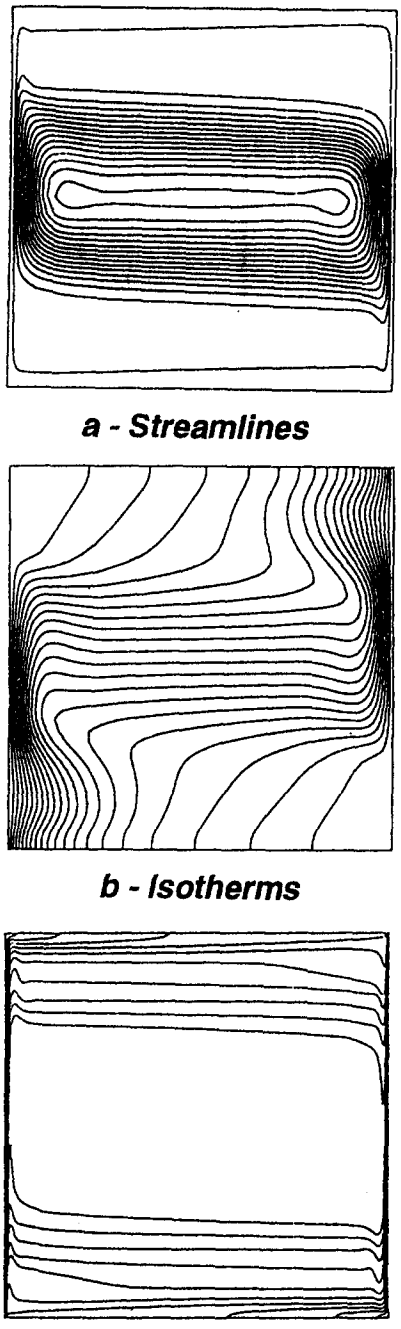

Fig. 5. Structure of the (a) velocity, (b) temperature and (c) concentration fields ($A = 1$; $Pr = 7$; $Le = 100$; $Gr_T = 10^5$; $N = 20$).

tom parts of the cavity. This is the purpose of the next section.

3. COMPOSITIONAL STRATIFICATION

When the density gradient inducing a natural convective flow depends only on one scalar field (temperature or concentration), it is well-known that, at a relatively high Rayleigh number, a temperature or concentration stratification takes place in the central part of the enclosure, as explained for instance by Worster and Leitch [12] in the thermal case. In order to get a better understanding of the situation described in the previous section, where the conductive heat transfer regime prevails at intermediate values of N/Le, we now analyse the influence of the thermal buoyancy term on the stratification when N varies.

Although the analysis developed in this section also concerns the study of the flow structure and the formation of multicellular flows, it is limited here to situations where only one recirculating flow is present in the cavity: we assume the existence of two boundary layers (the solutal and the thermal boundary layers), and that the concentration field is stratified in the top and bottom zones of the enclosure, and homogeneous in the central part.

3.1. *Influence of the governing parameters*

In the thermosolutal convective flows considered in this study ($Le > 1$), both diffusion processes are in competition, and because molecular diffusivity is much smaller than thermal diffusivity, species diffusion affects a smaller length scale. The strong solutal gradients are limited to thin layers close to the walls of the enclosure. On this scale, the temperature variations are generally small and heat transfer is essentially present on a length scale which is much larger than the solutal boundary layer. This may be schematically thought of as an outer flow due to the solutal buoyancy force and an internal thermal roll in the core region due to the thermal gradient (representation given in Fig. 6).

As a consequence of the presence of a thermally driven flow in the central part of the enclosure, the vertical variation in solute concentration is localized in the region between the thermal flow and the top (respectively, bottom) wall of the cavity. At high Lewis numbers, species diffusion is negligible: solute transport is mainly due to convection, and the top and bottom stratified regions consequently do not extend towards the centre, as it would happen in the absence of the thermal flow (purely solutal natural convection).

When the solutal buoyancy force is increased, it dominates over the thermal force and the solutal flow in the top and bottom regions has a larger extension. Through the continuity equation, the horizontal component of the velocity gets smaller, allowing for the diffusive term to become dominant over the advection term in this zone, which leads to the *vertical stratification in concentration*. Figure 7(a) displays the concentration profiles in the vertical midplane for $N = 20$ and different values of the Lewis number. It may be observed that increasing the Lewis number leads to the diminution of the height of the stratification zone; the solute diffusion length decreases and the thermal loop extends on a larger height. As a consequence, the concentration gradient ($\partial C/\partial z$) in the stratified zone

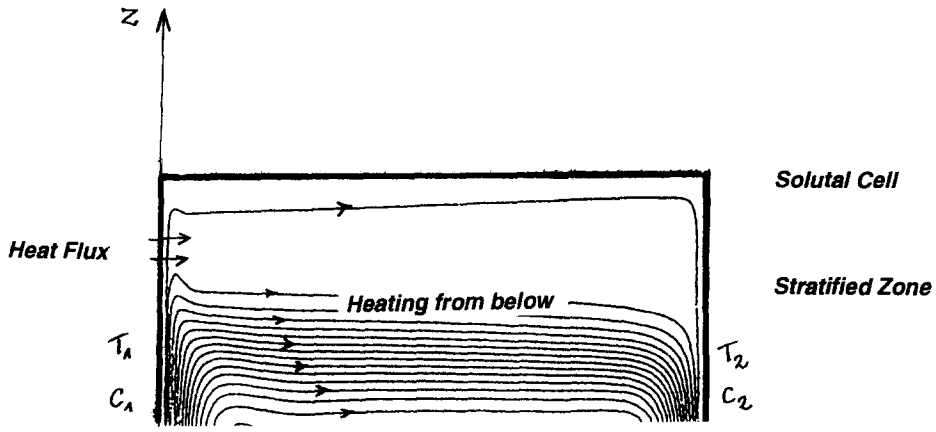

Fig. 6. Schematic representation of the structure of the top region of the enclosure. Inner thermal cell and top stratification zone.

increases. On the other hand, the height of the stratified zone increases with N [Fig. 7(b)], since the flow rate in the solutal boundary layer ($Q \sim \delta_S w_S \sim N^{1/4}$) increases with N, and also because the density is more sensitive to the solute concentration than to the thermal variations, thus the height of the thermal cell in the centre of the cavity is smaller. As a consequence, the fluid flow in the thermal cell is less intense, and it is not able to extract the same mass flux as at lower N values, so that the stratified zone extends on a larger height ($\partial C/\partial z$ is then smaller) which leads to a lower mass flux in the vertical direction.

3.2. *Estimation of the stratification height*

Let us consider the stratified zone in the upper part of the enclosure and let h^* be the height of this zone (Fig. 6). The velocity of the flow driven by the solutal buoyancy force is small and we may assume that the vertical variation of the concentration C is linear. The concentration flux in the vertical direction is supposed to be extracted by the thermal flow in the central part of the enclosure

$$\mathcal{J} \approx D\frac{C_1 - C_{avg}}{h^*} \tag{2}$$

where C_1 is the concentration specified at the hot wall. Let v_T be the average horizontal velocity in the thermal loop, the order of magnitude of v_T may be deduced from the thermal Rayleigh number based on the effective height of the thermal cell: $h_c = H - 2h^* = H(1-\xi)$

$$v_T \approx \frac{\alpha}{H} Ra_T^{1/2}(1-\xi)^{1/2}. \tag{3}$$

During the average time for a fluid particle to cross the width of the enclosure, $\tau \approx L/v_T$, the solute diffuses on a length $\eta \approx \sqrt{D\tau}$. The mass transfer rate between the stratified zone and the thermal cell is

$$\mathcal{J} \approx \Delta C^* \frac{\eta}{\tau}. \tag{4}$$

The system is in the steady-state if the local thermal buoyancy term balances the solutal force

$$\Delta\rho_C \sim \Delta\rho_T \tag{5}$$

with

$$\Delta\rho_C \sim \beta_S \Delta C^* \quad \text{and} \quad \Delta\rho_T \sim \beta_T \Delta T/2 \tag{6}$$

which finally leads to the following relation:

$$\xi(1-\xi)^{1/4} \sim 2N(LeA)^{-1/2} Ra_T^{-1/4}. \tag{7}$$

It is then possible to make an estimation of the minimum stratification height (ξ) for any steady-state situation defined by the parameters N, Le, A and Ra_T. This calculation is not valid any more if a recirculation cell takes place in the stratified zone (multicellular regime, see next section), or for small stratification heights, where the hypothesis of linear vertical variation of the solute concentration is not correct. So, in order to estimate the average heat transfer as a function of the height of the compositional stratification, we consider that heat transfer is mainly due to the thermal cell in the centre of the cavity, which excludes the multicellular regimes. Then, the heat transfer may be estimated on the basis of a Rayleigh number built on the effective height of the thermal cell

$$\overline{Nu} \sim Ra_{h_c}^{1/4} \sim \overline{Nu}_H(1-\xi)^{3/4} \tag{8}$$

where $\overline{Nu}_H$ is the average heat transfer obtained when the thermal cell occupies the whole height of the enclosure (low values of N). The estimation of the Nusselt number is then

$$\overline{Nu}/\overline{Nu}_H \sim (1-\xi)^{3/4}. \tag{9}$$

Figure 8 compares the estimated value of $\overline{Nu}$ using

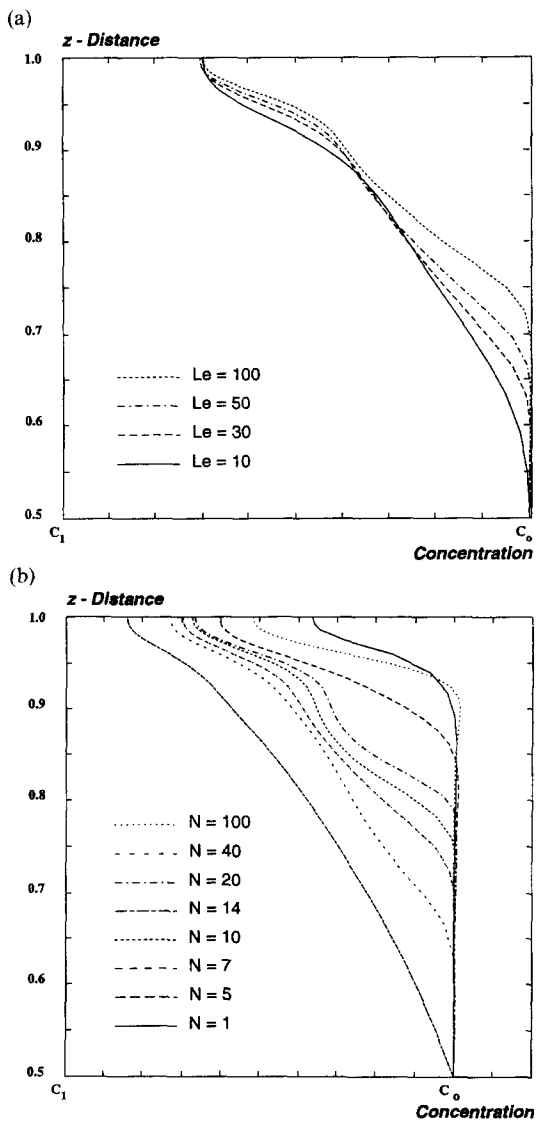

Fig. 7. Concentration profiles in the vertical midplane (top half of the enclosure). (a) Influence of the Lewis number, (b) influence of the buoyancy ratio ($A = 1$; $Pr = 7$; $Gr_T = 10^5$).

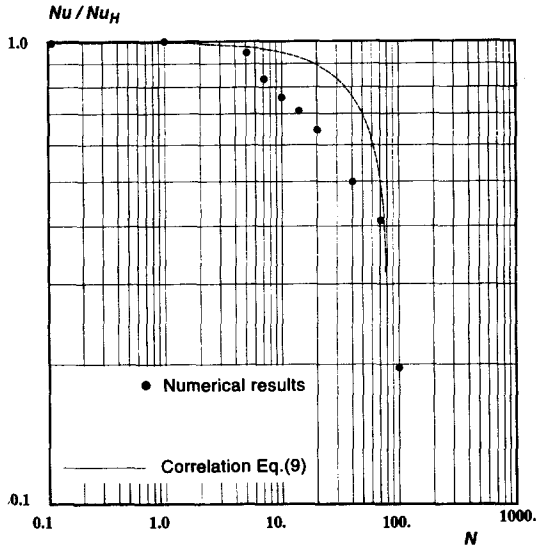

Fig. 8. Influence of the buoyancy ratio on the average Nusselt number ($A = 1$; $Pr = 7$; $Le = 100$; $Gr_T = 10^5$).

expression (9) (solid line) and the numerical results (symbols) at given values of Gr_T and Le for different values of N. The agreement is satisfactory and shows that the analysis leading to equation (9) may be used to estimate the decrease in heat transfer when N is increased at high Lewis numbers. Besides, at given Le and Gr_T, it is possible to determine the value of N corresponding to purely conductive heat transfer ($\overline{Nu} \sim 1$).

The above analysis gives some indications on the mechanisms that lead to the decrease in heat transfer associated with increasing buoyancy ratio, and on the influence of the different governing parameters. This analysis is however restricted to the situation where a compositionally stratified zone is present in the top and bottom part of the enclosure. The following section is dedicated to the study of the flow structure which results from the destabilization of these stratified layers and leads to a multicellular regime

4. FLOW STRUCTURE

As mentioned in the introduction, multicellular flows are obtained for moderate values of $|N|$ (N positive or negative), generally between 10 and 50. This structure comes from the fact that the thermal flow brings some fluid from the solutal boundary layer in a zone where the concentration is different. At a given height, the driving force is balanced by the buoyancy force, and the fluid flows horizontally towards the centre of the cavity, creating a recirculation.

This section is dedicated to the study of the conditions of existence of such a regime, and of the influence of the governing parameters (N, Le and Gr_T) on its formation. The mechanism is first studied in the steady-state, and then in the transient regime.

4.1. *Steady-state multicellular regime*

In the foregoing description, a 'multicellular regime' is a flow which presents more than one 'thermal cell' inside the main 'solutal cell' which develops close to the walls of the cavity. This definition excludes situations presenting a dominant solutal flow with a persistent thermal cell in the centre of the enclosure (see Section 3).

In order to study the conditions of formation of such multicellular structures, we first analyse the numerical results obtained when only one of the main parameters (Gr_T, Gr_S and Le) is varied: three different directions are thus explored. In a first step, Gr_S and Le are fixed at 2×10^6 and 100, respectively, and only the thermal Grashof number is allowed to vary from 10^4 to 4×10^5. The results are displayed in Fig. 9. For $N > 0$, different flow structures are observed, and Fig.

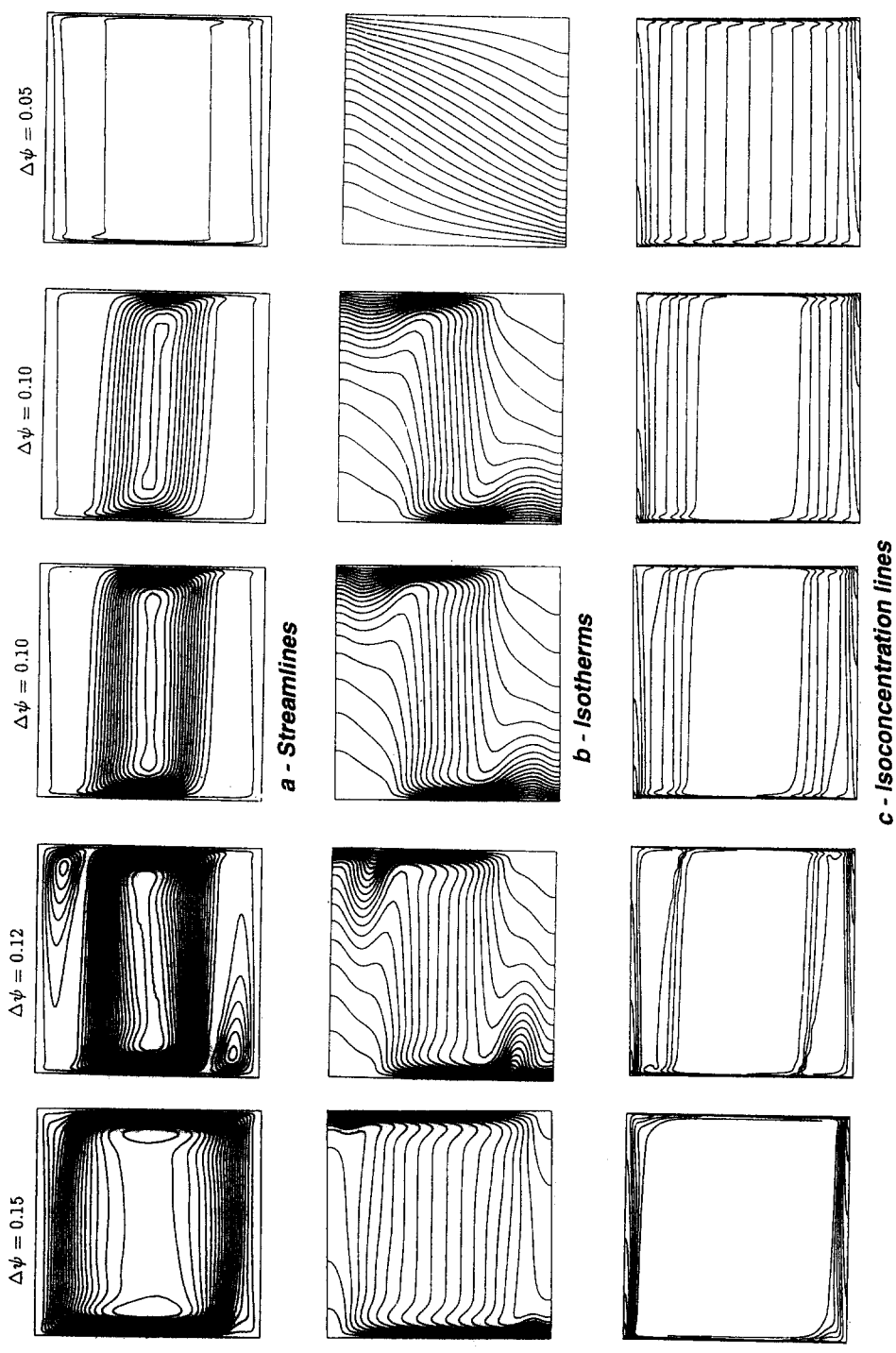

Fig. 9. Influence of the buoyancy ratio on the flow structure at a fixed Gr_S ($A = 1$; $Pr = 7$; $Le = 100$; $Gr_S = 2 \times 10^6$; $\Delta\phi = 0.05$; $\Delta\theta = 0.05$). (a) Streamlines; (b) isotherms; (c) isoconcentration lines.

9 shows the transition between the different situations:

(i) At low values of N ($N < 10$), the thermal buoyancy force is still relatively strong, and the flow is unicellular.

(ii) At moderate values of N, a multicellular structure is obtained, where several thermal cells are present in the centre of the cavity, inside a solutal recirculation loop close to the walls. The concentration inside each cell is uniform.

(iii) For higher N values, ($N > 20$), the solutal buoyancy force is dominating, and the flow is unicellular. This definition is different from the one given by some authors (e.g. Han and Kuehn [4]), since we consider that the case where a thermal cell still exists in the middle of the cavity belongs to this category.

The existence of a multicellular regime is due to the fact that the effect of temperature on density, although much less significant, is not negligible in comparison with the effect of concentration. It can be seen however that, for high N values, the thermal effect becomes negligible in the zone of compositional stratification close the horizontal walls. As mentioned in Section 3, the isotherms show that the heat transfer in this stratified zone is mainly conductive at high N, while the heat transfer due to the thermal effect only would be much more intense. These results show that the relative importance of the thermal and solutal effects directly determines the formation of a multicellular regime.

Similar conclusions are obtained when the thermal Grashof number is fixed and N varies with Gr_S. The results at $Le = 100$ and $Gr_T = 10^5$ are presented in Fig. 10. As the thermal buoyancy force is fixed, the height of the stratified zone increases with increasing Gr_S. These results show that, at a given value of the Lewis number ($Le \gg 1$), the value of N determines the presence of a multicellular structure. Let us underline that, for the same values of Le and N, and for different values of Gr_T (Fig. 11), the multicellular regime depends on Gr_T. At $Le = 100$ and $N = 20$, for $Gr_T < 10^4$, no multicellular regime is observed.

If one refers to the values of the parameters defined in the companion paper, N/Le and $N/Le^{1/3}$, it may be emphasized that the multicellular regime is obtained for $N/Le^{1/3} > 1$ and $N/Le < 1$, which means a situation where the solutal buoyancy force is dominating on the scale of the solutal boundary layer, while the thermal buoyancy force dominates on the scale of the thermal boundary layer (the so-called zone 2 in Fig. 3 of the previous paper). In both situations, the thermal cell persists in the centre of the cavity for a range of N which is much larger than the range corresponding to the multicellular regime.

The formation of a multicellular flow is related to the observations made in the previous section. It has been shown that, with increasing N, a stratified zone appears in the top and bottom regions of the enclosure, where a very weak horizontal flow takes place. When a fluid particle, initially at T_1 and C_1 moves horizontally from the left wall (hot and less concentrated) towards the cold and salty right wall, it gets colder and thus heavier as it gets closer to the right wall. The denser particle tends to go down along the wall and slows down when it penetrates in a more concentrated zone. As molecular diffusion is very weak, the local density difference increases more and more as the particle goes down. The solutal boundary layer at the right wall — more concentrated — prevents the fluid particle from getting closer to the wall, and then the particle moves away from the wall and heats up, creating a recirculation. This movement is stronger if the horizontal temperature gradient is higher, since the density variation due to the thermal effect becomes significant compared to the variation due to the solutal effect related to the vertical concentration stratification.

The multicellular regime is thus mainly due to the fact that the effect of the horizontal thermal gradient ($\partial\Theta/\partial x$) on the fluid density is of the same order of magnitude as the effect of the vertical compositional gradient in the stratified zone ($\partial\Phi/\partial z$), leading to the destabilization of the compositional stratification. It is clear that the increase of $\partial\Theta/\partial x$ may be obtained either by increasing ΔT (effect of the thermal Grashof number discussed previously), or by reducing the width L of the cavity; thus increasing the aspect ratio should facilitate the formation of a multicellular flow. This is illustrated by the results displayed in Fig. 12, where the parameters are identical, except for the aspect ratio A. The corresponding streamlines show that the number of cells is increasing for increasing A. The flow is constituted of three cells for $A = 2$ and five for $A = 8$.

There is an analogy with the destabilization of a stratified layer by lateral heating [5, 7, 13]. In the present situation, the phenomenon is more complex, since the height of the stratified zone is not given *a priori*, and it is not possible to estimate the solutal Rayleigh number based on this height, as it is done in the studies concerning the stratified zone [14, 15].

As a conclusion, a multicellular thermosolutal flow may be obtained if the solutal buoyancy force dominates over the thermal term, so that stratified zones may appear in the top and bottom regions of the cavity. These stratified zones will lead to secondary rolls if the stratified zone does not extend on the whole height of the enclosure, that is, if the thermal Grashof number is high enough for the lateral density gradient, due to $\partial\Theta/\partial x$, to destabilize the compositional stratification. This feature is different from the problem of destabilization by a lateral thermal gradient. In the present situation, the destabilizing effect is more difficult to obtain as the thermal Grashof number increases, since as a consequence of the stronger thermal buoyancy force, the thermal cell is more intense and the vertical extension of the stratified zone is

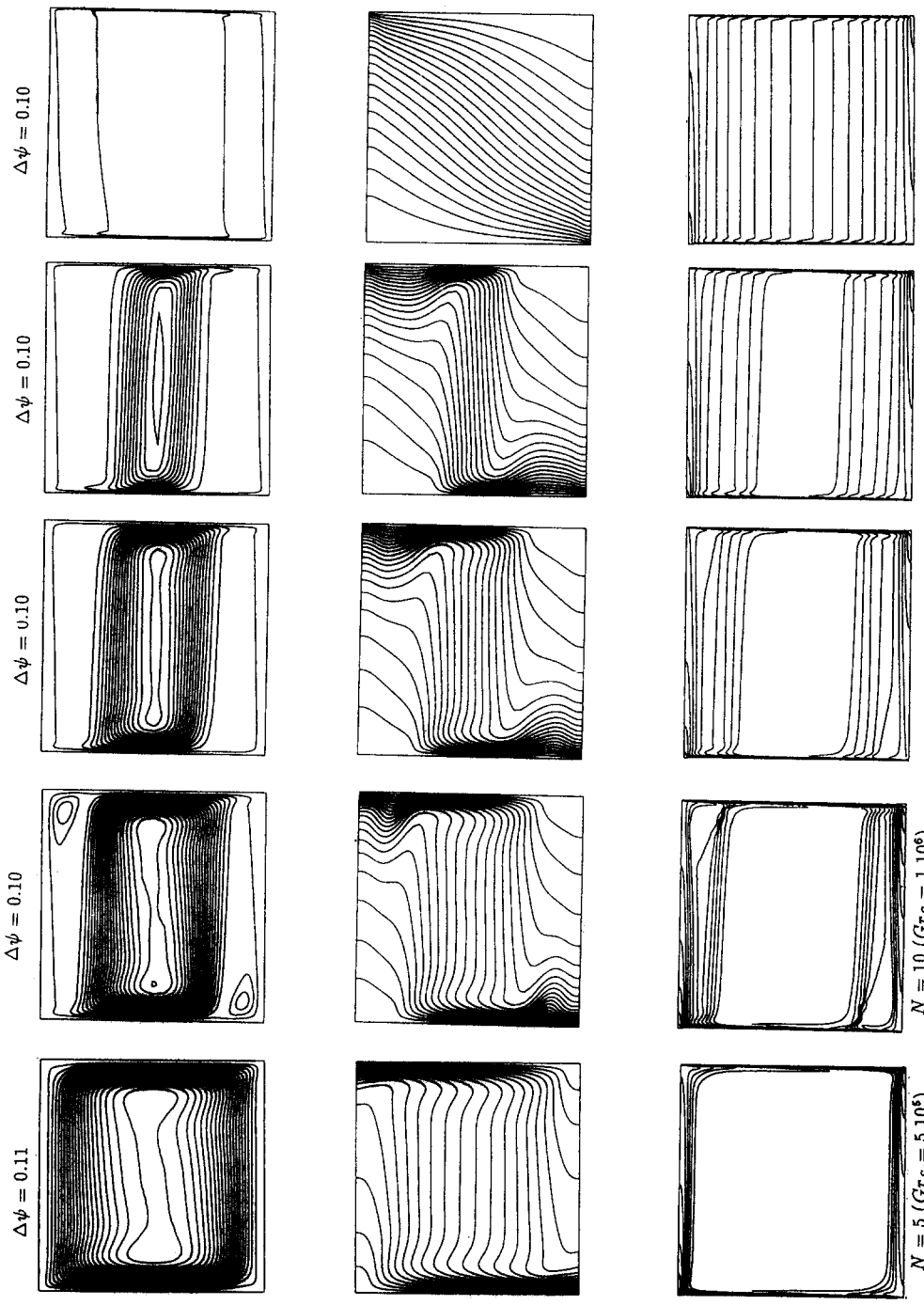

Fig. 10. Influence of the buoyancy ratio on the flow structure at a fixed Gr_T ($A = 1$; $Pr = 7$; $Le = 100$; $Gr_T = 10^5$; $\Delta\phi = 0.05$; $\Delta\theta = 0.05$). (a) Streamlines; (b) isotherms; (c) isoconcentration lines.

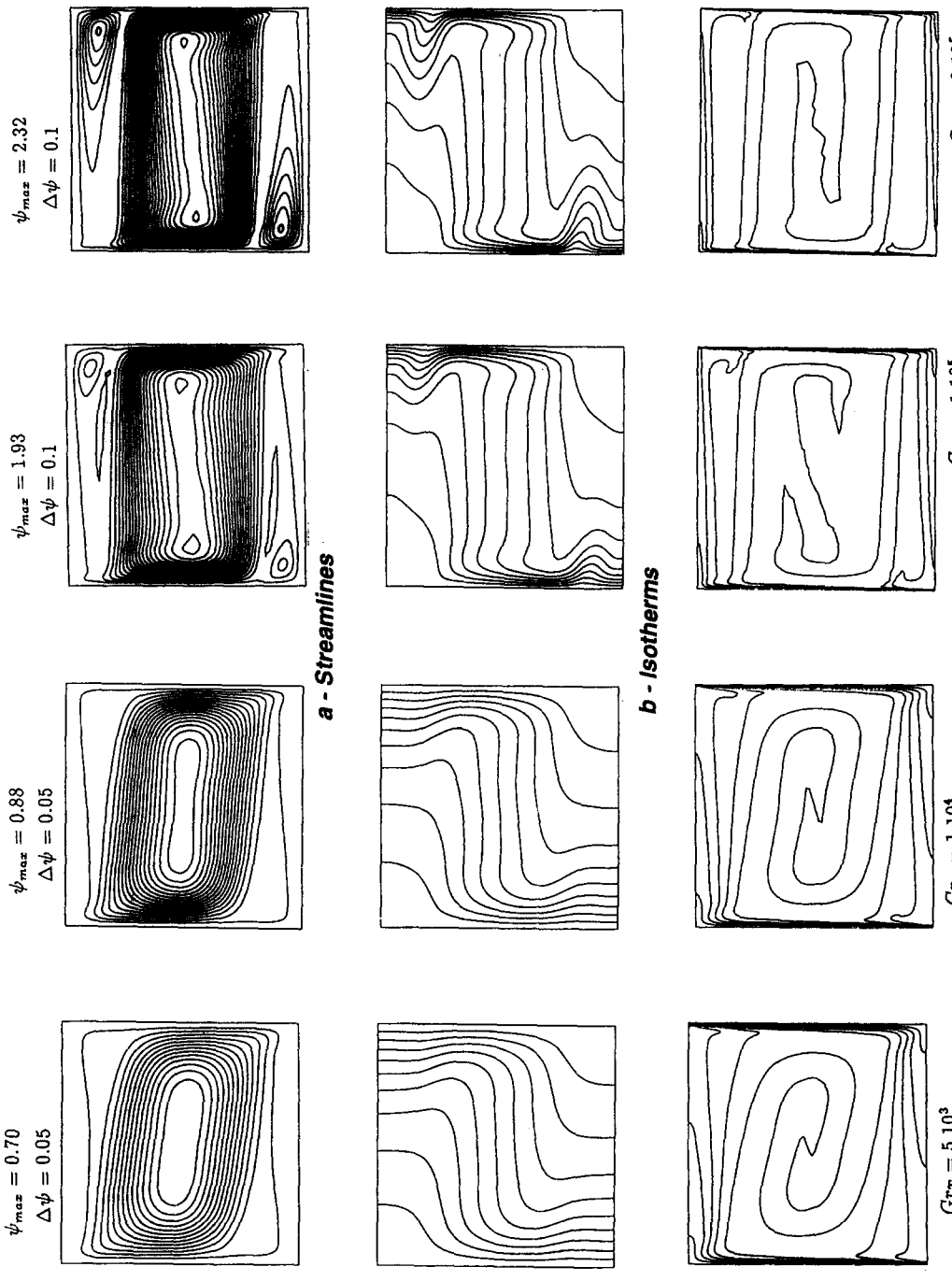

Fig. 11. Flow structure at a fixed buoyancy ratio ($A = 1$; $Pr = 7$; $Le = 100$; $N = 10$; $\Delta\phi = 0.05$; $\Delta\theta = 0.05$). (a) Streamlines; (b) isotherms; (c) isoconcentration lines.

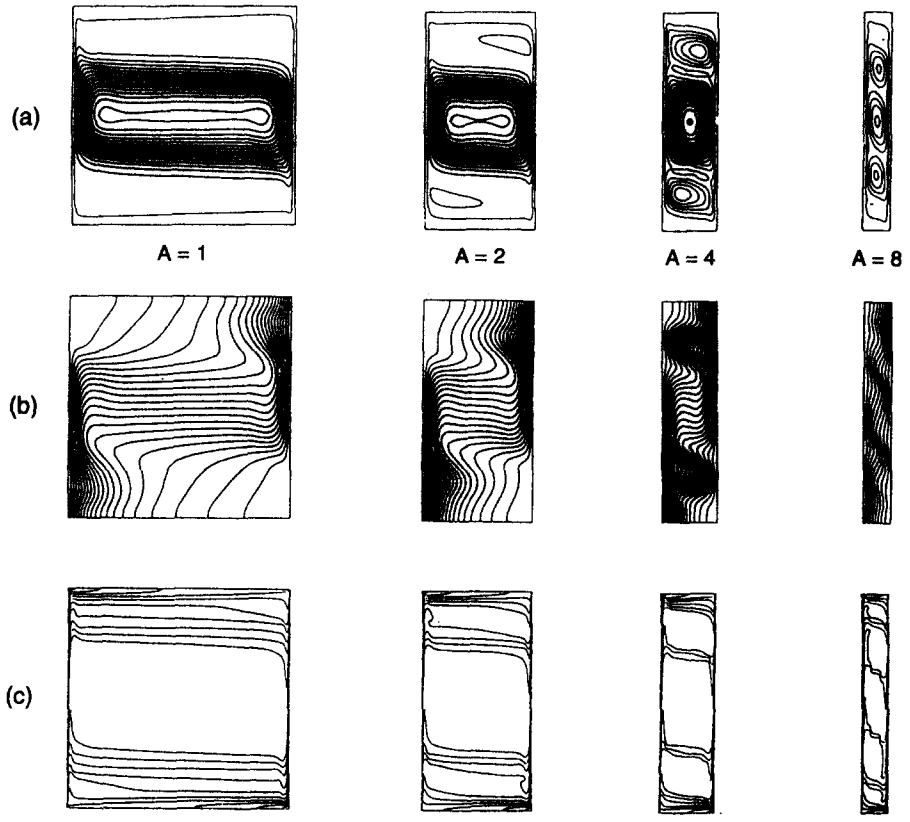

Fig. 12. Influence of the aspect ratio $A = 1, 2, 4$ and 8 ($Pr = 7$; $Le = 100$; $N = 20$; $Gr_T = 10^5$) ($\Delta\phi = 0.05$; $\Delta\theta = 0.05$; $\Delta\psi = 0.10$). (a) Streamlines; (b) isotherms; (c) isoconcentration lines.

reduced, which again stabilizes the stratified zone by increasing the vertical density gradient due to $\partial\Phi/\partial z$.

The compositionally stratified zone in the top half of the cavity is limited by the thermally driven flow at the bottom, and by the solutal flow on the other sides (see Fig. 6). The forces acting upon the compositionally stratified zone are the following:

(1) the thermal buoyancy force, due to the heating (cooling) of the stratified zone ($\partial\Theta/\partial x$) by the vertical walls;

(2) the shear stress due to the solutal flow, close to the top and vertical walls;

(3) the shear stress due to the thermal flow in the centre of the cavity at the bottom of the stratified zone;

(4) the thermal buoyancy force due to heating from below by the hotter fluid advected by the thermal cell.

According to the situation under consideration (opposing or cooperating buoyancy forces), these effects are either stabilizing or destabilizing. In the $N > 0$ range, the solutal flow in the boundary layers and in the stratified zones rotates in the same direction as the thermal flow. The effects are cooperating but the shear is relatively weak. The shear stress due to thermal buoyancy at the bottom of the stratified zone is stabilizing, but the heating from below is destabilizing.

In order to complete this analysis, it is necessary to estimate more accurately the mass flux, at the bottom of the stratified zone, that may be extracted by the thermal flow. This would give an estimate of the height of the stratified zone, and, from ($\partial\Phi/\partial z$), it would lead to the temperature gradient ($\partial\Theta/\partial x$) which is necessary to destabilize this zone, using the existing results on the sidewall instability of a stratified layer, as proposed by Tanny and Tsinober [14] or Jeevaraj and Imberger [15]. However these studies are basically different from the present situation in two main aspects: (1) they are concerned with situations where the compositional stratification is obtained in the absence of any thermal perturbation, and (2) they deal with destabilization of the initially stratified layer, with no consideration of the evolution towards a steady-state.

4.2. *Transient regime*

The results presented so far have been obtained in the steady-state. In this section, we wish to illustrate the transient establishment of the multicellular regime. We refer also to the study by Gau *et al.* [16] which deals with the experimental and theoretical analysis

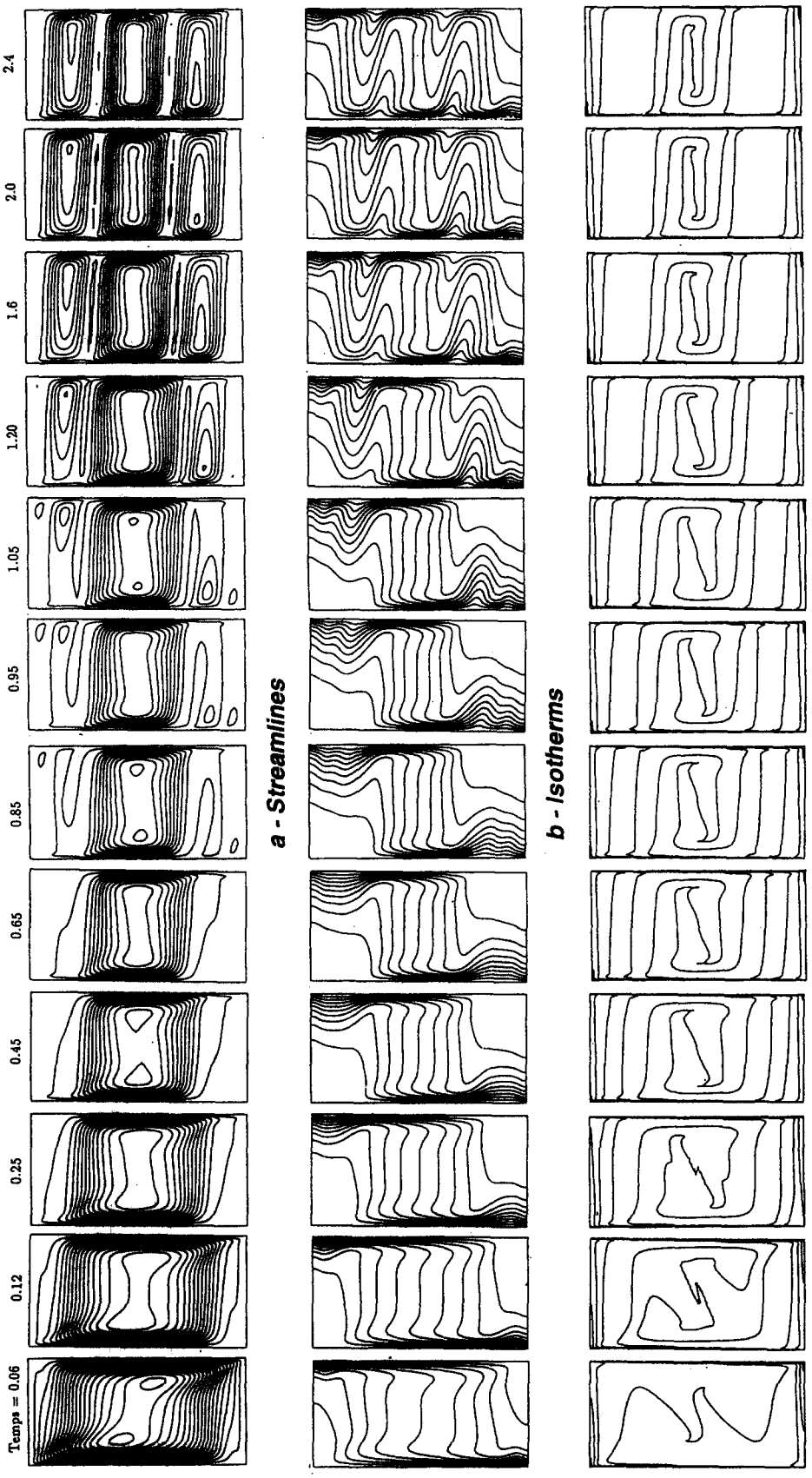

Fig. 13. Time evolution of the flow structure ($A = 2$; $Pr = 7$; $Le = 100$; $N = 20$; $Gr_T = 4 \times 10^5$) ($\Delta\phi = 0.10$; $\Delta\theta = 0.10$; $\Delta\psi = 0.20$). (a) Streamlines; (b) isotherms; (c) isoconcentration lines.

of the time development of such regimes. The reference test has been performed for $Pr = 7$, $Le = 100$, $Gr_T = 4 \times 10^5$, $N = 20$ and $A = 2$. The grid consists of 82 regularly-spaced nodes in the vertical direction and 47 nodes distributed in a geometrical progression in the horizontal direction. The dimensionless time step is 10^{-4}. The temperature and concentration conditions are imposed at the vertical walls of the enclosure, where the fluid is initially at rest, at the average temperature and concentration.

The time history of the streamlines is represented in Fig. 13(a), (respectively Figs. 13 (b and c) for the isotherms and isoconcentration lines). At the initial times, it can be noticed that the flow is mainly due to the thermal buoyancy force, as a consequence of the larger heat diffusivity. Then, solute stratification appears in the top and bottom layers close to the horizontal walls and grow towards the centre of the enclosure. This process leads to the formation of compositionally stratified zones, where the fluid velocity is very low. The extension of these zones increases with time and reduces the size of the initial thermal cell. The destabilization of those stratified zones leads to the creation of two secondary corotating cells corresponding to the onset of a multicellular regime. Indeed, the recirculating flow takes place in the vertically stratified zone when the concentration gradient, which decreases with time may be destabilized by the horizontal temperature gradient. When the solution tends towards steady-state, this multicellular structure remains stable.

5. CONCLUSION

This study is dedicated to the analysis of heat transfer and flow structures for natural convective flows in a binary fluid due to cooperating thermal and solutal buoyancy forces. It has been shown that the heat transfer characteristics at high Lewis numbers in such systems has a special behaviour, since it decreases with increasing buoyancy ratio. This is due to the formation of stratified zones in the top and bottom parts of the cavity where the fluid velocity is very small, and the heat transfer mainly due to diffusion. The estimation of the orders of magnitude of the height of the stratification zone and of the decrease of the heat transfer is given.

The destabilization of the stratified zones may lead to the formation, under some conditions, of a multicellular regime, and the thermosolutal convective flows may be classified in four different regimes:

(1) unicellular regime, where the flow is dominated by the thermal effect (low N);

(2) multicellular regime, where the thermal and the solutal effects are comparable in the central part of the cavity (moderate N),

(3) flow globally driven by the solutal buoyancy force, with a persisting thermal cell in the centre,

(4) unicellular regime, where the solutal force is dominating (high N).

The study of the formation of multicellular flows in the enclosure shows the influence of the different governing parameters. It is assessed that the formation of a multicellular structure is obtained when the horizontal temperature gradient is sufficiently strong compared with the vertical concentration gradient. These flows are obtained for moderate values of the buoyancy ratio N. We have shown that, on one hand, the increase of the thermal Grashof number Gr_T at fixed N and Le values, helps the formation of thermosolutal cells, and that, on the other hand, the formation of a multicellular flow is easier for higher values of the aspect ratio. Although we are still not able to define a criterion in terms of these parameters, allowing us to define *a priori* whether the flow is mono- or multicellular, the above analysis shows that the multicellular regime is present when both the solutal and the thermal effects are dominating on their own scale (i.e. the solutal or thermal boundary layer). This is typically defined by the range

$$\frac{N}{Le} < 1 \quad \text{and} \quad \frac{N}{Le^{1/3}} > 1. \tag{10}$$

Acknowledgement—The calculations have been performed on the C98 Cray supercomputer at IDRIS (the CNRS Computer Center in Orsay), in the frame of project 94-0336.

REFERENCES

1. C. Bénard, D. Gobin and J. Thévenin, Thermosolutal natural convection in a rectangular enclosure: numerical results, *Heat Transfer in Convective Flows ASME National Heat Transfer Conf.* Philadelphia, pp. 249–254. ASME, New York. (1989).
2. T. F. Lin, C. C. Huang and T. S. Chang, Transient binary mixture natural convection in square enclosures, *Int. J. Heat Transfer* **33**, 287–299 (1990).
3. C. Béghein, F. Haghighat and F. Allard, Numerical study of double-diffusive natural convection in a square cavity, *Int. J. Heat Mass Transfer* **35**, 833–846 (1992).
4. H. Han and T. H. Kuehn, Double diffusive natural convection in a vertical rectangular enclosure. Part I: experimental study, Part II: numerical study, *Int. J. Heat Mass Transfer* **34**, 449–460, 461–471 (1991).
5. J. W. Lee and J. M. Hyun, Time-dependent double diffusion in a stably stratified fluid under lateral heating, *Int. J. Heat Mass Transfer* **34**, 2409–2421 (1991).
6. Y. Kamotani, L. W. Wang, S. Ostrach and H. D. Jiang, Experimental study of natural convection in shallow enclosures with horizontal temperature and concentration gradients, *Int. J. Heat Mass Transfer* **28**, 165–173 (1985).
7. J. Lee, M. T. Hyun and K. W. Kim, Natural convection in confined fluids with combined horizontal temperature and concentration gradients, *Int. J. Heat Mass Transfer* **31**, 1969–1977 (1988).
8. O. V. Trevisan and A. Bejan, Combined heat and mass transfer by natural convection in a vertical enclosure, *J. Heat Transfer* **109**, 104–112 (1987).
9. P. Ranganathan and R. Viskanta, Natural convection

in a square cavity due to combined driving forces, *Numer. Heat Transfer* **14,** 35–59 (1988).
10. J. M. Hyun and J. W. Lee, Double-diffusive convection in rectangle with cooperating horizontal gradients of temperature and concentration, *Int. J. Heat Mass Transfer* **33,** 1605–1617 (1990).
11. R. Bennacer, Convection naturelle thermosolutale: simulation numérique des transferts et des structures d'écoulement, Thèse de Doctorat de l'Université Pierre et Marie Curie (1993).
12. M. G. Worster and A. M. Leitch, Laminar free convection in confined regions, *J. Fluid Mech.* **156,** 301–319 (1985).
13. T. L. Bergman and A. Ungan, A note on lateral heating in double diffusive systems, *J. Fluid Mech.* **194,** 175–186 (1988).
14. J. Tanny and A. B. Tsinober, The dynamics and structure of double-diffusive layers in sidewall-heating experiments, *J. Fluid Mech.* **196,** 135–156 (1988).
15. C. G. Jeevaraj and J. Imberger, Experimental study of double-diffusive instability in sidewall heating, *J. Fluid Mech.* **222,** 565–586 (1991).
16. G. Gau, K. H. Wu and D. J. Jeng, Layer growth process of transient thermosolutal convection in a square enclosure, *Int. J. Heat Mass Transfer* **35,** 2257–2269 (1992).